

IMPERIAL COLLEGE LONDON  
DEPARTMENT OF MATERIALS

MATE50003 ENGINEERING PRACTICE  
**Interim Report**  
30th May 2024

Group: A01  
Project Manager: Dr Jonathan Rackham

*Marcus Chien  
Freddie Johnson  
Folake Olusanya  
Jeanne Tay  
Nathanael Tjoa  
Felix Watson*

# Contents

<b>1</b>	<b>Introduction</b>	<b>2</b>
<b>2</b>	<b>Characterisation</b>	<b>3</b>
2.1	Experimental details . . . . .	3
2.2	Gear sample . . . . .	4
2.2.1	Results . . . . .	4
2.2.2	Discussion . . . . .	4
2.3	Handle Grip . . . . .	5
2.3.1	Results . . . . .	5
2.3.2	Discussion . . . . .	5
2.4	Chuck Jaw . . . . .	6
2.4.1	Results . . . . .	6
2.4.2	Discussion . . . . .	7
2.5	Green Casing . . . . .	7
2.5.1	Results . . . . .	7
2.5.2	Discussion . . . . .	8
<b>3</b>	<b>Recommendations</b>	<b>8</b>
3.1	Gear . . . . .	8
3.2	Chuck Jaw . . . . .	9
3.3	Handle Grip . . . . .	9
3.4	Green Casing . . . . .	10
3.5	Summary . . . . .	10
<b>4</b>	<b>Budget Spend Report</b>	<b>11</b>
<b>5</b>	<b>Appendix</b>	<b>12</b>
<b>6</b>	<b>Contributions</b>	<b>12</b>

## Executive Summary

This report displays the process by which a FADAKWALT 8212A Cordless Drill Driver has been broken down into key components and then to the materials used. This leads to recommendations and agreements concerning the materials used for this drill in maximising its performance for desired use. Characterisation experiments were set out and prepared for the various materials in the studio's previous report. It is then highlighted how these were executed for each type of material: PA6-GF30, TPE, and two steels. The purpose being a discussion of our findings to determine exactly what the materials of the components are and how they were processed. The studio succeeded in this by determining the processes for every material, that the grip was a Thermoplastic Vulcanize (TPV) of EPDM and PP blend, the gears being a porous, low-carbon, martensitic steel and the chuck jaw being a low Manganese alloyed steel. From this, previous hypotheses made about each material could be answered, such as how was the desired hardness was achieved in the chuck jaw? Therefore, suggestions were made on whether to change the material completely, improve its alloying or processing methods, or to keep the selection as is and agree with what the provider has chosen. These findings will be what we present to the rest of our company as reasons for and against certain materials and components included in the ideal drill. Each test did, however, cost money and as per our characterisation plan we were able to stay under budget. In the end, £3,725 was spent out of a possible £5000. Despite having to repeat DSC experiments a few times for no gain, SEM/EDX were overestimated in our plan for how many sessions were required meaning both balanced out. In the future, a better understanding of exactly why and how different experiments are going to be performed would be optimal for budget and time saving.

## 1 Introduction

The FADAKWALT 8212A Cordless Drill Driver presents itself as a multi functional tool used for a variety of applications on small to mid-range DIY projects. It features a maximum torque of 20Nm and offers a 20+1 adjustable clutch, that is, 20 discrete torque settings with the addition of a drill mode for which the drill operates at its maximum torque and speed settings. This range allows for precise control and versatility, enabling users to select the optimal torque for different tasks, thus preventing over-tightening and reducing the risk of damaging screws or work surfaces.

This device is powered by a 12V lithium-ion (Li-ion) battery, known for its high energy density and large cyclability, ensuring prolonged operational periods and reduced charging intervals. The absence of a power cord enhances maneuverability and allows for use in locations without immediate access to electrical outlets whilst compromising on the power which may be needed for larger applications. The Li-ion battery is more than sufficient for the target market. The drill's bright green color scheme enhances visibility, facilitating easy identification in cluttered work environments. These design elements underscore the tool's suitability for both DIY users and seasoned professionals, ensuring adaptability across various drilling and driving tasks.

Priced at £29.99, the FADAKWALT 8212A Cordless Drill Driver sits around the middle of the cordless drill driver market. With other products ranging from £139.99, such as the BOSCH Home and Garden Cordless Combi Drill,<sup>[1]</sup> to £16.59 for the Flintronic Electric Screwdriver Cordless.<sup>[2]</sup> The FADAKWALT 8212A therefore places itself as a combination of reliability and great design with cost efficiency.

To better understand the balance that has been struck in the material selection, this report outlines the characterization of the gears, chuck grip, casing, and hand grip and investigates alternatives. These components are critical to the drill's functionality and user experience. The gears are essential for optimal torque and speed, affecting the tool's efficiency and lifespan. The chuck grip ensures secure holding of drill bits, reducing slippage and enhancing safety. The casing provides structural integrity and durability, protecting internal components from environmental factors. The hand grip enhances user comfort and control, reducing fatigue during prolonged use. Characterizing these materials allows for targeted improvements in durability, safety, ergonomics, and performance, ensuring the drill meets user needs effectively.

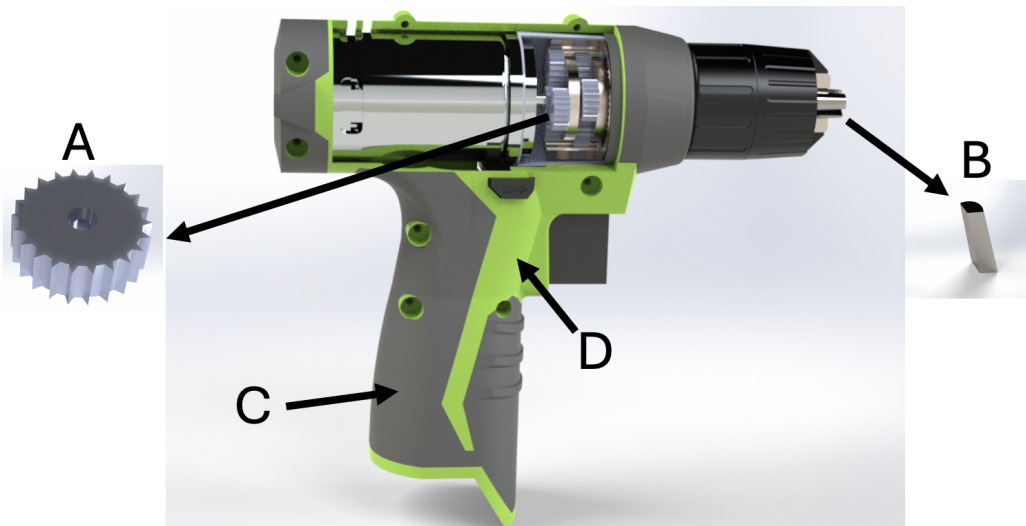


**Figure 1: 3D Render of the FADAKWALT 8212A with the labelled key components for characterisation; A) Gear, B) Chuck jaw, C) Handle grip and D) Green casing.**

## 2 Characterisation

### 2.1 Experimental details

**X-ray Diffraction Spectroscopy (XRD)** was performed on the gear, chuck jaw and handle grip samples on a Bruker D2 Phaser, spinning on. The X-ray source was a copper  $K\alpha$  source with a nickel filter, 30 kV 10 mA. For all samples the parameters were set as  $2\theta$ : 20°-100°, step size: 0.035°, step time: 0.9s and the peaks were indexed using the 'Match!' software.<sup>[3]</sup> All samples were mounted on bakelite and ground using 320 grit sand paper and then taken out of the mount. Notably, the chuck jaw sample had 2 surfaces orientated at 45° to the ground surface which may lead to uncharacteristic peaks in the data.

**Light Optical Microscopy (LOM)** was employed on an Olympus BX51 fluorescence optical microscope, utilising the full range of the microscope. Only reflectance light modes were used, Nital etchant preparation for metal chuck and gears, no preparation needed for casing and grip.

**Fourier Transformed Infrared (FTIR) Spectroscopy** was conducted on a ThermoScientific Nicolet iS10. All samples were flattened before being placed on the sample compartment and secured by the anvil.

**Scanning Electron Microscopy/Energy-Dispersive X-ray Spectroscopy (SEM/EDX)** was performed on a JOEL JSM-6010PLUS/LA with an operating voltage of 20kV, working distance between 18mm-20mm, and spot size of 50SS. A gold coating was applied onto the casing and grip as both samples are non-conductivity. The images were further analyzed using ImageJ software.<sup>[4]</sup> The EDX mapping image for all of the sample were not used in the final report however the elemental compositional data was still used.

**Densimetry** was performed on a scale. A sample's weight was measured in air and then in water, and using Equation 2.1, their density was calculated. Where  $\rho$  = the density of the sample,  $A$  = the weight of the sample in air,  $B$  = weight of the sample in liquid,  $\rho_0$  = density of water and  $\rho_L$  = density of air ( $0.0012g/cm^3$ ). While the weight was being measured, the slides were closed to prevent fluctuations in weight.

$$\rho = \frac{A}{A + B}(\rho_0 - \rho_L) + \rho_L$$

**Hardness** Chuck jaw and gear hardness was tested using a Zwick Roell DuraScan 80. A grid testing method was employed, with each test point spaced 0.5mm apart in all directions to minimize the influence of adjacent tests on the hardness results. Samples were polished and ground to ensure a flat surface, thereby improving the accuracy of the hardness data. (Note that polishing was done manually so the sample may not be perfectly flat)

## 2.2 Gear sample

### 2.2.1 Results

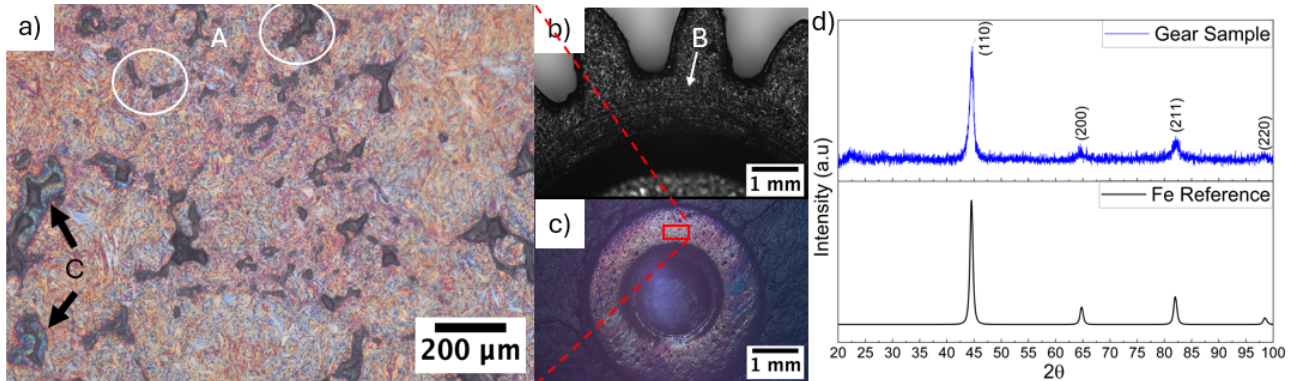


**Figure 2: VLM and XRD data of the sample gear.** a) VLM image of the etched gear surface showing a porous martensitic structure at 50x magnification with labelled pores (A) and alloyed oxides (C) b) VLM image of unetched gear showing machining surface finish (B) at 1.25x magnification c) VLM of gear surface at 1.25x magnification d) XRD analysis of gear (blue) with reference data (black).

XRD analysis in Fig. 1d of the gear sample found it most similar to pure iron. Sub-surface level VLM uncovered a fine lath microstructure with a large number of pores (Fig. 1A) and a very small number of inclusions such as cementite. The presence of darker regions in Figure 1C was also noted around a couple of the pores. VLM on the gear surface level highlighted concentric circles which appear as markings from a lathe machine.

### 2.2.2 Discussion

The irregular shape and uniform distribution of pores is indicative of the use of powder metallurgy during processing methods.<sup>[5]</sup> The presence of sinter necks suggests a further stage of sintering typically at  $\approx 600^{\circ}\text{C}$  which can improve the hardness and density of the iron.<sup>[6]</sup> The formation of the needle-like structure is a definitive indicator of the martensitic phase, we can conclude some level of carbon doping must be present up to  $\approx 0.6\%$ .<sup>[7]</sup> This is somewhat contradictory to the XRD analysis which implies that the sample is pure iron. However, both pure iron and martensite have similar XRD patterns, with martensite having some peak broadening around the (200) and (211) peaks which is observed in Fig. 1d.<sup>[8]</sup> The darker regions in Fig. 1C is believed to be oxide regions commonly occur through the 'internal getter' effect which is associated with low alloyed steels processed above  $\approx 700^{\circ}\text{C}$ . The 'internal getter' effect describes the movement of oxygen from iron oxides to form oxides with alloying elements.<sup>[9,10]</sup> This relatively larger processing temperature than the sintering stage can be attributed to the martensitic phase transformation which requires heat treatment above  $\approx 900^{\circ}$  for an initial transition to austenite.<sup>[11]</sup> This would then be followed by rapid cooling resulting in the formation of the lath martensite structure observed in Fig. 1a.<sup>[11]</sup> Through visual inspection of Fig. 1a, the martensite grains mostly have an area of approximately  $10 - 50 \mu\text{m}^2$ , this indicates the austenite temperature prior to rapid cooling must be around the range of  $900 - 1000^{\circ}\text{C}$  (and not at excessive heating  $> 1000^{\circ}\text{C}$ ).<sup>[12]</sup> To obtain the geometry of the gear, two common processes are used in industry of sintered components for different applications; powder metallurgy (PM) and metal injection moulding (MIM). PM is a cheaper alternative to MIM, offering lower equipment and production costs but has limitations on the components with advanced geometries. MIM gives higher precision and can work with more complex geometries.<sup>[13]</sup> One of the key difference between the two is the much larger initial particle sizes used in PM which creates more porosity within the sample. The combination of the porosity in Fig. 1A, the non-uniform dispersion of alloying elements seen from oxide formation in Fig. 1C and the presence of lay roughness in Fig. 1B indicating some post casting machining (likely on a lathe) all strongly support the theory that PM must have been used.<sup>[13]</sup> Post casting machining is commonly used on PM components to reach tighter tolerances which is mostly not required in MIM.<sup>[13]</sup>

Given the outer context of the drill being a combination of reliability and great design with cost efficiency, the use of PM processing is a clear choice which represents this design philosophy. PM components have great durability, hardness and strength if sintered but also possess the ability to be mass produced reliably and precisely at a cheap rate.<sup>[14]</sup>

## 2.3 Handle Grip

### 2.3.1 Results

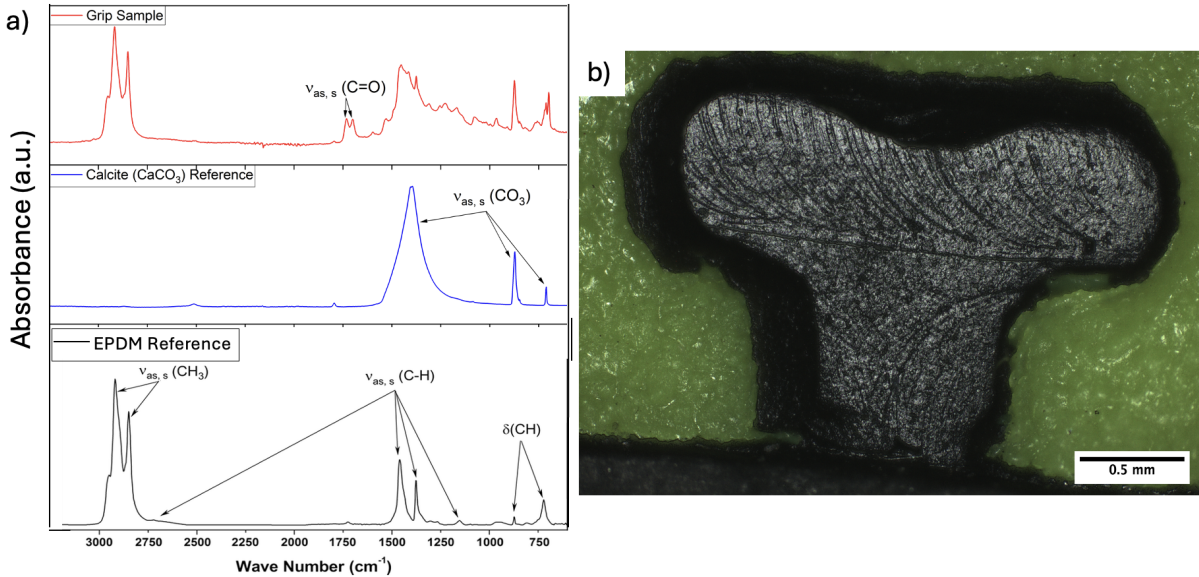


**Figure 3: FTIR and VLM data of the grip sample.** a) FTIR of grip sample (red), reference calcite (blue) and reference EPDM (black) b) VLM of interface between the casing and the grip handle.

In the Poly(ethylene-propylene-diene monomer) (EPDM) FTIR reference data, the bands originating from the symmetric and asymmetric stretching vibrations of the methyl and methylene groups ( $\nu_{as}$ ,  $\nu_s$ ,  $(CH_3)$ ) are, respectively, centred at  $2950\text{cm}^{-1}$  and  $2800\text{cm}^{-1}$ . The stretching vibrations of the CH groups ( $\nu_{as}$ ,  $\nu_s$ ,  $(CH)$ ) are localised at  $1154\text{cm}^{-1}$ ,  $1375\text{cm}^{-1}$ ,  $1460\text{cm}^{-1}$ , and  $2723\text{cm}^{-1}$ . The bending vibrations ( $\delta(CH)$ ) of the CH groups of the double bond can be observed at  $725\text{cm}^{-1}$  and  $808\text{cm}^{-1}$ . In the Calcite ( $CaCO_3$ ) FTIR reference data, peaks are found at  $718\text{cm}^{-1}$ ,  $875\text{cm}^{-1}$  and  $1425\text{cm}^{-1}$  corresponding to out of plane bending and asymmetrical stretching vibration peaks of  $CO_3$  ( $\nu_{as}$ ,  $\nu_s$ ,  $(CO_3)$ ), respectively. It is clear to see that the grip sample FTIR data is the addition of the Calcite data with the EPDM data. More peaks were also identified as symmetric and asymmetric stretching vibrations of the  $C=O$  groups ( $\nu_{as}$ ,  $\nu_s$ ,  $(C=O)$ ) which are, respectively, centred at  $1730\text{cm}^{-1}$  and  $1700\text{cm}^{-1}$  which may come from many sources. Fig. 1b shows the mechanical bond between the rubber handle and the green casing of the component. These indentations are present throughout the handle at regular intervals. The XRD analysis of the grip in Fig. 4 exposed a broad peak around  $20^\circ$  and calcite crystalline phase.

### 2.3.2 Discussion

Amorphous materials do not have a regular crystal structure and therefore produce broad diffuse patterns without sharp peaks in XRD.<sup>[15]</sup> Furthermore, the broad peak seen in Fig. 4 is believed to show the presence of an amorphous polymer. This would explain the calcite found in XRD analysis which is commonly used as a polymer non-reinforcing filler in the plastic industry.<sup>[16]</sup> Adding calcite eases the polymer extrusion and also lowers the cost.<sup>[17]</sup> It enhances the heat resistance, stiffness, hardness and provides abrasion resistance of the polymer.<sup>[16]</sup>

FTIR in Fig. 3a supported the presence of calcite initially identified in the XRD analysis. It also uncovered the amorphous polymer as EPDM rubber – a synthetic rubber made from ethylene, propylene and diene monomers. The peaks in the FTIR data corresponding to  $C=O$  bond vibrations are thought to be contamination from the oil-based lubricant in the gearbox which had transferred due to poor handling of the sample.

Material markings in accordance with the ISO18064<sup>[18]</sup> standard on the drill indicated that the polymer used

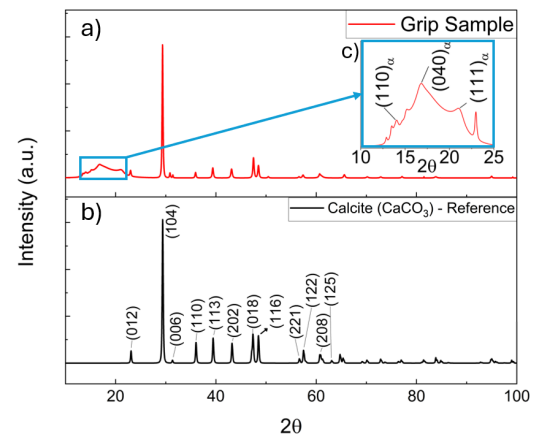


**Figure 4: XRD patterns** of the grip sample (a) with a reference calcite spectrum indexed(b). c) XRD pattern of grip across  $10^\circ - 25^\circ$  range with PP peaks indexed.

for the handle grip was a TPE. EDPM in itself is an elastomer and not a TPE. Thermoplastic vulcanisates (TPVs) are a particular family of TPEs, which are produced via dynamic vulcanisation of non-miscible blends of a rubber and a thermoplastic.<sup>[19]</sup> As a result, the products obtained consist of crosslinked rubber particles dispersed in a thermoplastic matrix, combining the elasticity of rubber with the processability of thermoplastics, making it ideal for applications such as handle grips. Polypropylene (PP) is considered as one of the most efficient thermoplastics for EPDM vulcanisation due to their similar chemical structure which facilitates physical interactions at their interface and is most commonly used in industry.<sup>[20]</sup> It is therefore reasonable to assume our sample is a PP/EPDM blend. The FTIR spectrum of PP has multiple sharp peaks around  $2900\text{ cm}^{-1}$  and many other peaks around the fingerprint region, most notably a large one at  $1378\text{ cm}^{-1}$ .<sup>[21]</sup> These peaks closely match with  $\nu_{as,s}(CH_3)$  and  $\nu_{as,s}(CO_3)$ , respectively, which may be why they were not identified. Upon further inspection of the amorphous region of the XRD pattern in Fig. 4c peaks were found which corresponded to monoclinic  $\alpha$ -PP.<sup>[22]</sup> It should be noted that because the amorphous halo is so large, not all PP peaks were able to be indexed and therefore this is not a conclusive result and only suggests the presence of PP. Increasing rubber content increases the height of the amorphous halo and decreases the height of the crystalline peaks.<sup>[23]</sup> Estimating the amount of crystallinity of the PP/EPDM blend as 10% from the ratios of amorphous and crystalline areas under the XRD pattern allows the use of the "rule of mixtures" to estimate the PP content to be  $\approx 10\%$ .<sup>[23]</sup> The rubber component of the EPDM/PP blend provides elastic recovery and softness for the user so, based on the large EPDM content, a clear design choice has been made here to prioritise the users experience.<sup>[24]</sup>

The presence of mechanical bonding between the green casing and EPDM/PP blend in Fig. 3b is indicative of an overmoulding process.<sup>[25]</sup> This process technique is broadly categorized into two types: (i) multi-material moulding and (ii) insert moulding. Multi-material injection involves the injection of the first material, substrate, into the mould, and then the subsequent material is injected onto the solidified substrate.<sup>[26]</sup> On the other hand, insert overmoulding requires a previously prepared insert placed into the mould cavity, and then polymeric material is injected directly on it.<sup>[27]</sup> Although it is difficult to identify which may have been used for the processing of this component, multi-material moulding stands out as the most cost-effective due to its high level of automation and high productivity while guaranteeing a high level of quality.<sup>[28]</sup>

The question set out in the preliminary report: "Is the tactility adequate for its use case?" can therefore be answered from our characterisation. EPDM/PP blends are commonly used for hand held equipment, at low strain rates they do not deform but at high rates they do deform which causes the grip to mold around the geometry of the users hand - thereby increasing tactility, amongst other things, making them suitable for the application.<sup>[29]</sup>

## 2.4 Chuck Jaw

### 2.4.1 Results

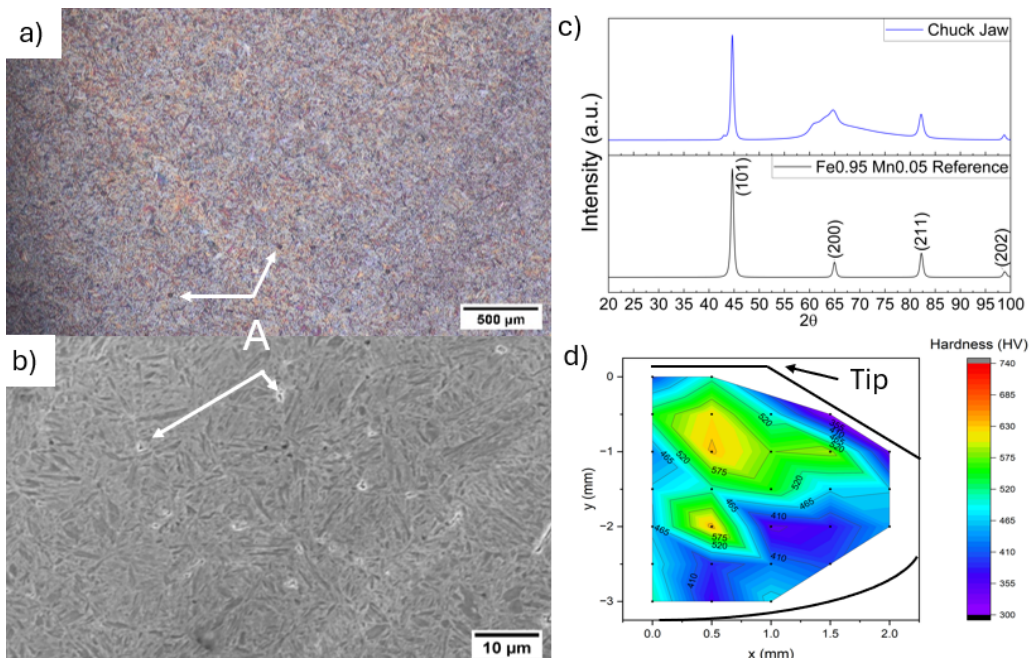


**Figure 5: VLM, XRD and hardness heatmap of chuck jaw sample.** a) VLM image of the etched chuck jaw surface at 50x magnification b) SEM image of the etched chuck jaw sample at x1500 magnification. Both showing regular, small inclusions (A) c) XRD of chuck jaw (blue) with reference data (black) d) Hardness heat map of a Vickers test with cross section outline in black and tip labelled.

XRD analysis of the chuck jaw sample, in Fig. 5c, showed the closest match was Fe0.95 Mn0.05. VLM images from Fig. 5a then showed the very fine grain structure with small dark inclusions most likely to be cementite (Fig. 5A). The fine grain structure can be separated into a dual-phase whereby one is the brown matrix and the other are the fine, brighter regions. These potentially indicate ferrite and martensite respectively.<sup>[30]</sup> Upon further inspection in Fig. 5b, SEM showed inclusions through the charging effect, build-up of electrons due to non-conductive material, again thought to be cementite. Meanwhile, small darker spots also appeared, indicating that fewer secondary electrons were emitted suggesting very small defective holes. The EDX data obtained from the same sample, Table 1 showed the provisioned Mn of the XRD as well as very small amounts of F and Sr. The heat map generated then describes a trend in hardness whereby it decreases as one moves further from the tip and outer surface. A maximum value of 635 on the Vickers scale was measured just below the tip.

## 2.4.2 Discussion

Due to the specific shape and steel of the jaw required for its function, closed-die forging was most likely the process used to form the steel as forged steel is usually stronger than cast. Closed-die will also achieve the desired shape.<sup>[31]</sup> Although, to achieve the needle-like structure shown in the VLM, the material would have to contain a low carbon content, in turn being a martensitic steel, similar to the gears in Section 2.2. The carbon content, 0.06-1.15wt%,<sup>[30]</sup> can then be an explanation for the formation of cementite shown in the SEM image of Fig. 5b. One could suggest that this contradicts with the XRD pattern found, however the martensite has similar peaks as well as broadening about the (200) peak which corresponds to Fig. 5c.<sup>[12]</sup>

This martensitic structure is achieved through rapid cooling from the austenitic + ferritic phase of the steel. Rapid cooling is required from a high temperature as the phase change of austenite to martensite is not thermally activated. This is because the nucleation barrier is dominated by the strain energy associated with the FCC to BCT transformation.<sup>[32]</sup> The starting temperature for martensite formation (Ms) is usually around 500 °C,<sup>[33]</sup> but quenching starts from around 900 °C.<sup>[30]</sup> To increase this driving force, Manganese (Mn) can be alloyed to stabilise the austenite phase to lower temperatures.<sup>[30,34]</sup> Therefore, increasing the likelihood of all the pre-existing austenite turns to martensite therefore maximising hardness. Another benefit of Mn as an alloying element is that it strengthens the ferrite upon solidification,<sup>[30,34]</sup> in turn enhancing the physical properties of the steel. This is then proven for its function by Fig. 5d. The tip end of the jaw will be where hardness is most needed as it will be holding the drill bit and should not wear throughout use. This suggests the tip was quenched first and therefore cooled the quickest leading to the most martensite present as well as the highest hardness.

## 2.5 Green Casing

### 2.5.1 Results

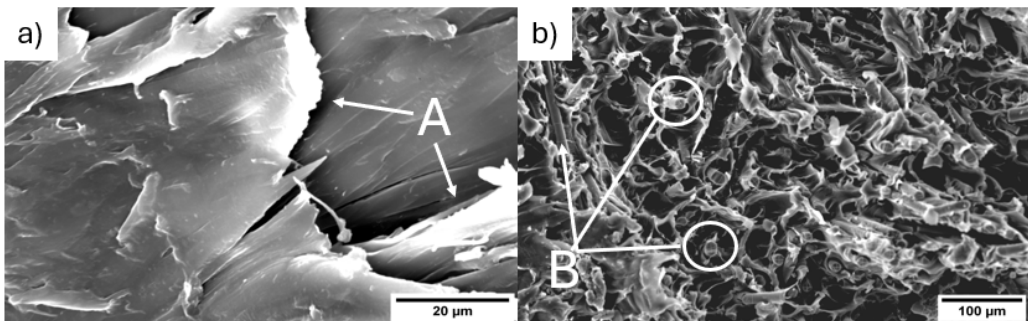


**Figure 6: SEM images of green casing** a) surface image with charging features (A). b) cross section image showing glass fibers (B) in the polymer matrix

SEM images of the green casing cross section (Fig. 6b) exposed the glass fibres (GF) in the polymer matrix (Fig. 6B). SEM on the surface of the sample showed the polymer matrix, no glass fibres where visible. Charging was also noted in Fig. 6a due to uneven gold sputtering. EDX mapping of both samples highlighted the larger ratio of organic to inorganic elements whilst also indicating the presence of potential additives in the form of transition metals. The atomic weight percentages of these elements can be found in Table 2.

**Table 1:** EDX elemental composition data taken from Fig. 5b

Formula	Atom%	Sigma
Fe	92.57	0.28
Mn	2.40	0.26
C	3.62	0.13
F	1.02	0.07
Sr	0.22	0.33

**Table 2:** EDX elemental composition data taken from Fig. 6a (surface) and 6b (cross-section)

Formula	Surface		Cross-section	
	Atom%	Sigma	Atom%	Sigma
C	78.34	0.14	86.31	0.18
O	15.41	0.52	7.87	0.62
Au	0.89	0.89	1.83	0.71
Si	0.04	0.16	3.19	0.12
Cr	0.73	0.46	-	-
Fe	2.36	0.59	-	-
Nb	0.89	0.54	-	-
Al	-	-	0.76	0.11
Ca	-	-	1.41	0.2

### 2.5.2 Discussion

Material markings in accordance with the ISO16396<sup>[35]</sup> standard on the drill indicated that the composite used for the green casing was Nylon 6 - 30% Glass fiber (PA6-GF30). EDX mapping (Fig 7) across Fig. 6b showed a high concentration of Si, Ca, and Al atoms on the GF, as expected. Ca and Al are commonly used as network modifiers and intermediates, respectively, increasing its working range and improving mechanical and chemical properties.<sup>[36]</sup> The absence of these GF associated elements on the surface SEM (Fig. 6a) indicates a level of directionality to the GF within the matrix. Fig. 6b also showed the full length of some of the GFs, exposing the short fibre nature of the reinforcements commonly referred to as milled GF.<sup>[37]</sup> The directionality and use of milled GF leads to the conclusion that injection moulding was used during processing. Injection moulding creates alignment of GF with the direction of the matrix flow which explains the directionality.<sup>[38]</sup>

To get the green colour of the component one common colorant for nylon-6 is phthalocyanine green pigment.<sup>[39]</sup> It has high colour strength, good weathering properties and it compatible with chemically stable in nylon-6.<sup>[39]</sup> When preparing an injection mold polymer batch, usually only around 3 – 5% of the pellets will be that of colorant<sup>[40]</sup> which may explain why some constituent elements of phthalocyanine green pigment; Cu and N, where not identified in the EDX mapping so further work should be conducted to confirm it's presence. The concentration of phthalocyanine green pigment in plastic colouring formulations is also expected to be low as the component has a light green colour. The low concentrations of Cr, Fe and Nb are thought to be contaminants from the injection mold die as they are elements usually associated with steel which is the material commonly used for injection molding dies.<sup>[41]</sup>

The identification of injection molding for the green casing and overmolding for the grip handle lends itself into the theory that multi-material injection molding was used to produce this component.

From this characterisation, the question set out in the preliminary report can be answered: "What is the structure of the glass fibres within polyamide casing?". It is clear that the glass fibres are milled with a directional alignment parallel to the flow of the nylon-6 matrix in the injection molding.

## 3 Recommendations

### 3.1 Gear

Hardness, toughness and fatigue life are some of the most crucial properties when designing an optimised gear. The presence of pores throughout the gear sample compromises these mechanical properties of the gear by up to a factor of 4.<sup>[42]</sup> Altering the synthesis of the PM metal could offer a cheap and quick improvement which does not require further expenditure to be spent on new machinery. One such method could be to use a finer powder for the initial press and sintering stage. The percentage of coarse particles in the powder ( $> 150\mu\text{m}$ ) is inversely proportional to the hardness, density and UTS<sup>[43]</sup>

As mentioned in our preliminary characterisation plan, a hardness to cost ratio would be desirable to understand how both the performance could be increased while staying cost effective. Manufacturers only give a quote depending on your desired mould and components, rather than listing prices. However, as further machining is required for PM metal,<sup>[13]</sup> apart from altering the synthesis of the metal, the company should look into the difference in cost when buying the gears in bulk rather than internally using PM machinery and having to pay employees to machine the gears to the desired pitch. This could also potentially increase the quality of the

metal and so the performance. Having said that the addition of glass fibre would improve wear resistance of gears so one could argue the exactly use of the green casing material could be recommended which would provide extensive cost reduction.<sup>[44]</sup>

Other materials could also be considered for the gears such as ceramics or polymers.

Zirconia ( $ZrO_2$ ) and Alumina ( $Al_2O_3$ ) are two examples of ceramic based materials which are currently being used for gears.<sup>[45]</sup> Ceramics gears, similarly to PM components, require sintering for the densification of the material at temperatures up to  $1100^{\circ}C$ . Ceramic gears are extremely hard which can lead to excellent wear resistance, they are resistant to chemical corrosion and are very light weight.<sup>[46]</sup> However, the big disadvantage with ceramics is the price. The raw materials are very expensive and due to the extremely hard nature of the material after the sintering stage, diamond tools are required for machining.<sup>[47]</sup> If a company wanted to invest into the machinery to process ceramic gears, although the start up costs would be large, the manufacturing costs would be moderate.

On the other end of the spectrum are polymer based gears. There are two polymers used on a large scale for usage in gears: polyamides such as Nylon 6 and Nylon 6,6 and acetol.<sup>[48]</sup> Although polymers generally cannot handle as much load as metals, they offer a much cheaper alternative to PM gears. Given that the casing of our drill is made partially from nylon 6 this seems like an easy cost-reduction choice for the manufacturer. Having said that the addition of glass fibre would improve wear resistance of gears so one could argue the exactly use of the green casing material could be recommended which would provide extensive cost reduction.<sup>[44]</sup> The main disadvantage of polymer gears is the limit of the torque which could be applied to them due to there weaker nature comparatively with PM steels. As well as this it can be difficult to reach dimensional tolerances and they are much more susceptible heat.<sup>[48]</sup>

Multiple different sintering methods could also be employed. From the characterisation of the gear sample it was understood that a conventional or 'free' sintering method was used. This has long processing times which require elevated heat for a long period of time causing larger processing costs to the manufacturer. Some other possible sintering techniques such as pressure-assisted sintering, spark plasma sintering (SPS) or hot isostatic pressing could be used as an alternative.<sup>[49]</sup> Although each of these deserve full consideration in there own rights, the momentary application of more intense pressure or temperature will result in a decrease of porosity and manufacturing times.<sup>[50]</sup> Thereby increasing the hardness and fatigue resistance of the gear as well as reducing the cost.

### 3.2 Chuck Jaw

When thinking about the chuck jaw for its function, the closed-die process seems sensible, for the supplier of the chuck, to achieve its desired shape repeatedly and to a better quality than casting. Extrusion could also be used; however, this creates a uniform cross-section down the rod meaning that further machining would be required.<sup>[51]</sup> The alloying elements are the key to this part. The carbon wt% will determine the hardness of the martensite and so, the steel. The Manganese included aids in the formation of martensite and strengthening of the ferritic phase.<sup>[30,34]</sup>

Many commercial steels have at least two alloyed elements for various property enhancements, not just Manganese. Most can add to what the Mn is already providing to the metal, for example Nickel (Ni) is an austenitic stabiliser, like Mn. However, Nickel is listed as 13.9 \$/kg<sup>[52]</sup> whereas Manganese is 1.82 \$/kg.<sup>[52]</sup> In reference to the hypothesis question, when planning our characterisation: "How is the desired hardness achieved?" The manufacturers solution is Mn as an alloying element. Properties such as corrosion resistance are not needed and it also minimises cost, in turn covering all needs for the chuck's function. Not many recommendations can be made for the low Manganese alloy steel used by the supplier who manufactured the chuck. This is expected as the chuck is a bought in part and readily available indicating the makeup is quite standardised.

### 3.3 Handle Grip

The physical benefits of TPV show that, due to the crosslinking of the elastomer present, there is a change in viscoelasticity.<sup>[53]</sup> As the TPV goes from liquid to solid, the long-time behaviour improves<sup>[54]</sup> making it's physical properties comparable to that of silicone. Meaning that the physical properties are a big improvement on non-cross linked polymers while keeping thermoplastic properties.<sup>[55]</sup> On the other hand, silicone grips are highly resistant to temperature extremes due to their thermosetting nature<sup>[56]</sup> and provide a comfortable feel, but they can be more expensive to process and may not offer the same level of durability as TPVs. Overall, TPVs offer a balance between user comfort, durability, and cost-effectiveness, making them a suitable choice for handle grips in various applications.

We conclude that characterisation confirms that our sample is a TPV, leveraging the properties of both EPDM

rubber and PP to achieve the desired performance characteristics. This is a good choice for the grip handles used in drills. It offers the best balance between its softness/elasticity and its manufacturability, in turn leading to user safety. Cost reductions can also be implemented by introducing calcite fillers without significant effect on the TPV's properties. We would highly recommend the use of TPV as grips in the final design through an over-moulding process.

### 3.4 Green Casing

Polyamide/short glass fibre composite is widely used due to their high strength-to-weight ratio and high durability with excellent wear resistance. However, it has its disadvantages. The cost of Polyamide 6 with glass fibre is relatively high compared to other plastics, and it requires precise control during the moulding process, which can complicate manufacturing. Glass fibre percentage can also be increased to improve stiffness, hardness and decrease in shrinkage and warpage from the injection moulding process.<sup>[57][58]</sup>

Polymer nanocomposites reinforced by montmorillonite (MMT) show considerable enhancements in mechanical, barrier, thermal and flammable properties at very low filler loadings.<sup>[59]</sup> The combination of one such nano scale filler with a micro scale filler such as chopped glass fiber used the green casing would improve the mechanical properties of the material. Given the montmorillonite is found in sediments and clays, it is somewhat readily available so this could offer a cheap alternative to increase the lifespan of the drill.<sup>[60]</sup>

In terms of manufacturing process, a higher melt temperature and volume flow rate parameter during injection moulding is proven to increase fatigue life and mechanical properties.<sup>[61]</sup> Polyamide 6,6 can be considered for its lower cost and similar stiffness although they have lower temperature resistance and wear resistance.<sup>[62]</sup> A certain degree of mineral filler can be added to make the component cheaper and favourably modify properties such as stiffness, tensile strength, heat distortion and mouldability. However, it is a trade off on decreasing mechanical properties and elongation to break.<sup>[63]</sup>

As an alternative, Polycarbonate (PC) can be considered. PC is known for its extremely high impact resistance and durability.<sup>[64]</sup> However, the cost of Polycarbonate is higher than Polyamide 6, and it requires higher temperatures for moulding, typically around 280-310 °C.<sup>[64]</sup> The typical temperature range for the PA6-GF30 is generally between 260 °C to 280 °C. Another potential alternative is Acrylonitrile Butadiene Styrene (ABS). ABS is more cost-effective than Nylon 6 and offers good impact resistance and toughness. It is also easier to mould than Nylon, making the manufacturing process less complicated. On the downside, ABS has lower heat resistance compared to Nylon and is not as strong as glass fibre-reinforced Nylon. ABS is typically processed through injection moulding at temperatures between 200-250 °C.

### 3.5 Summary

**Gears:** Powder metallurgy is a clear choice for the processing of these gears, balancing great properties with mass manufacturing ease. Considering that, improvements can be made by altering the synthesis by using a finer powder – leading to better hardness, density and UTS. This change whilst improving properties would not require new machinery, saving costs.

**Chuck Jaw:** We concluded that the current low Mn alloy steel used is suitable, offering the needed hardness without unnecessary cost increases. A closed-die manufacturing process is recommended for achieving consistent and high-quality shapes.

**Handle Grip:** TPVs provide excellent balance in physical properties, making them comparable to silicone. While silicone grips offer superior temperature resistance and comfort, TPVs are most cost-effective and durable, making them a strong recommendation for the final design. Overmoulding remains the most suitable manufacturing process.

**Casing:** PA6 with short GFs are a good choice but come at a higher cost and require precise moulding control. GFs prove to be the best choice for reinforcements in the nylon. Strong candidates for alternatives are polycarbonates or ABS, with polycarbonate having superior properties, and ABS being the most cost-effective option.

## 4 Budget Spend Report

The total expenditure for the characterisation techniques amounted to £3,725, as detailed in Table 3, leaving a remaining balance of £1,400. Notably, conductivity testing incurred a minimal cost of £100. Each technique's cost was documented carefully to ensure transparency and accountability. The budget was strategically allocated across various tests to ensure comprehensive analysis while maintaining financial efficiency. SEM and EDX received the highest allocations due to their critical roles in material characterization, providing key information. Lesser allocations were made to FTIR/UV-Vis, hardness testing, and LOM, reflecting their supportive but essential roles in backing up the hypothesis. Metal preparation and DSC were also prioritized for their specific contributions to the analysis.

Comparing the actual expenditure to the predicted spending from a previous report, the predicted total was £3,425, while the actual expenditure was slightly higher at £3,725. Notable differences include higher costs for SEM/EDX and metal preparation in the actual spending. The predicted costs for hardness testing and FTIR/UV-Vis were accurate, whereas the actual cost for conductivity testing and DSC was not initially predicted but was included in the final budget.

We found that some experiments, like DSC, were overestimated in terms of the number of times we needed to perform them. On the other hand, some tests were carried out that we had not expected to do initially. In the end, it balanced out well, and we only spent a little above the predicted amount. However, the use of DSC was not as useful as anticipated, and we were not able to obtain the data we were expecting such as the  $T_g$  and  $T_m$  of the TPE. The time and money spent on performing the DSC could have been utilised better, and therefore in the future this can be avoided by better preparing for experiments and determining suitable parameters beforehand.

This allocation strategy allowed for a balanced approach, ensuring all necessary techniques were employed effectively within the budget. The budget was managed efficiently, resulting in a remaining balance of £1,400. Future studies could improve costs further by reassessing the necessity of less critical tests. These measures will enhance budget efficiency and ensure that financial resources are used optimally to achieve the project's objectives.

Technique	Cost £/hr	Sessions	Time (hr)	Net Cost (£)
SEM/EDX	750	1	1	750
XRD	500	2	1	500
FTIR/UV-Vis	500	1	0.5	250
Hardness	500	2	1	500
Metal Prep	250	3	1.5	375
LOM	250	2	1	250
Etchants	50	1	1	50
DSC	500	4	2	1000
Conductivity	100	1	0.5	50
Total				3,725
Remaining				1,275

**Table 3:** Spending across the characterisation stage.

## 5 Appendix

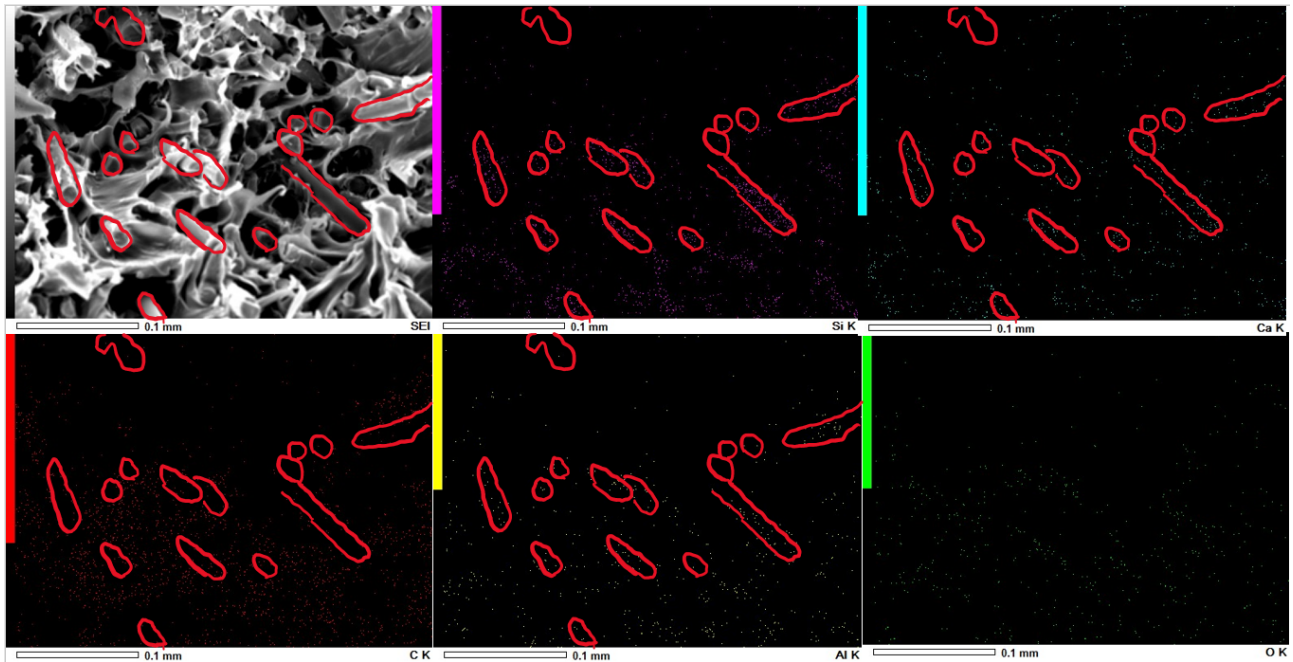


Figure 7: EDX mapping of PA6-GF30 cross section with glass fibres outlined

## 6 Contributions

**Felix:** Gear Characterisation, Introduction (part), Formating, Figures, Experimental details (Main)

**Marcus:** Introduction (part), Motor/battery/gearbox writing, Recommendations(Supporting research), Budget, Experimental details (Supporting)

**Nathanael:** PA6-GF30 Characterisation, Recommendations

**Freddie:** Chuck Grip Characterisation, Summary, Experimental details, Recommendations

**Jeanne:** TPE Characterisation, Recommendations, Proof reading

## References

- [1] ScrewFix - BOSCH GSB 18V-90 C 18V LI-ION COOLPACK BRUSHLESS CORDLESS COMBI DRILL - BARE, <https://www.screwfix.com/p/bosch-gsb-18v-90-c-18v-li-ion-coolpack-brushless-cordless-combi-drill-bare/>, Accessed: 27-05-2024.
- [2] Flintronic Electric Screwdriver Cordless, 3.5N·m Max Torque Electric Screwdriver Kit with 25 Accessories, 3.6V/1300mAh Rechargeable Power Drill Driver, with USB Cable LED Light for Home Office DIY, [https://www.amazon.co.uk/Flintronic-Electric-Screwdriver-Cordless-Accessories/dp/B08DHSGTP7/ref=asc\\_df\\_B08DHSGTP7?tag=bingshoppinga-21&linkCode=df0&hvadid=80127005179679&hvnetw=o&hvqmt=e&hvbmt=be&hvdev=c&hvlocint=&hvlocphy=&hvtargid=pla-4583726553188604&th=1](https://www.amazon.co.uk/Flintronic-Electric-Screwdriver-Cordless-Accessories/dp/B08DHSGTP7/ref=asc_df_B08DHSGTP7?tag=bingshoppinga-21&linkCode=df0&hvadid=80127005179679&hvnetw=o&hvqmt=e&hvbmt=be&hvdev=c&hvlocint=&hvlocphy=&hvtargid=pla-4583726553188604&th=1), Accessed: 27-05-2024.
- [3] D. H. Putz, K. Dr. K. Brandenburg GbR, Match! - Phase Analysis using Powder Diffraction, Version 3.x, Crystal Impact.
- [4] C. A. Schneider, W. S. Rasband, K. W. Eliceiri, NIH Image to ImageJ: 25 years of image analysis. Nature Methods, 9(7), 671–675. doi:10.1038/nmeth.2089.
- [5] T. Ping, X. Kuangdi, *The ECPH Encyclopedia of Mining and Metallurgy* 2024.
- [6] O. BERGMAN, *Department of Materials and Manufacturing Technology CHALMERS UNIVERSITY OF TECHNOLOGY* 2011.
- [7] M. Lionel, *Marks' standard handbook for mechanical engineers*, McGraw-Hill, 1978.
- [8] T. Liu, L. Liang, D. Raabe, L. Dai, *Journal of Materials Science Technology* 2023.
- [9] H. Danninger, R. de Oro Calderon, C. Gierl-Mayer, *Institute of Materials Minerals and Mining* 2018.
- [10] C. Gierl-Mayer, R. de Oro Calderon, H. Danninger, *JOM* 2016.
- [11] M. Banerjee, *Comprehensive Materials Finishing*, Chapter: 2.1 Fundamentals of Heat Treating Metals and Alloys, 7 Elsevier Inc, 2017.

- [12] Z. Babasafari, A. V. Pan, F. Pahlevani, R. Hossain, V. Sahajwalla, M. du Toit, R. Dippenaar, *Journal of Materials Science Technology* **2020**.
- [13] Metal Injection Molding vs Powder Metallurgy, <https://www.zcmim.com/mim-vs-pm/>, Accessed: 27-05-2024.
- [14] P. Ramakrishnan, *Advances in Powder Metallurgy*, Woodhead Publishing, **2013**.
- [15] C. Chandrasekaran, *Anticorrosive Rubber Lining*, Chapter: 12 - Rubbers Mostly Used in Process Equipment Lining, Plastics Design Library, **2017**.
- [16] Fillers > Calcium Carbonates (ground), <https://polymer-additives.specialchem.com/product-categories/additives-fillers-calcium-carbonates-ground/>, Accessed: 29-05-2024.
- [17] Calcite Use In Plastic Industry, <https://monomex.com/research-and-development/know-how/calcite-use-in-plastic-industry>, Accessed: 27-05-2024.
- [18] Thermoplastic elastomers — Nomenclature and abbreviated terms, Standard, International Organization for Standardization, Geneva, CH, **2022**.
- [19] K. De S, A. K. Bhowmick, *CiNii Research* **1990**.
- [20] M. ISHIKAWA, M. SUCIMOTO, T. INOUNE', *Journal of applied polymer science* **1996**.
- [21] J. Fang, L. Zhang, D. Sutton, X. Wang, *Journal of Nanomaterials* **2012**.
- [22] W.-Z. Wang, Q.-H. Wu, B.-J. Qu, *Chem. Res. Chinese Univ. Vol. 20 No. 1* **2004**.
- [23] L. Farhang1and, R. Bagheri, *Materials Performance and Characterization* **2014**.
- [24] Why Choose EPDM Rubber Surfacing for Your Next Flooring Project, <https://www.rubcorp.com/choosing-epdm-rubber-surfacing/>, Accessed: 29-05-2024.
- [25] Overmolding Design Guide: Essential Tips for Dual-Material Products, <https://proleantech.com/overmolding-design-guide/>, Accessed: 29-05-2024.
- [26] B. R., R. P. K., K. J. G., *Express Polymer Letters* **2019**.
- [27] T. Donderwinkel1, M. van Drongelen2, S. Wijskamp, : *Advances in Polymer Processing* **2020**.
- [28] S. Boßhammer, *Organosilicon Chemistry V: From Molecules to Materials* **2003**.
- [29] G. Harih, B. Dolšák, *Applied Ergonomics* **2014**.
- [30] (PDF) Study of solidification cracking during laser welding in advanced high strength steels: A combined experimental and numerical approach, [https://www.researchgate.net/publication/334672402\\_Study\\_of\\_solidification\\_cracking\\_during\\_laser\\_welding\\_in\\_advanced\\_high\\_strength\\_steels\\_A\\_combined\\_experimental\\_and\\_numerical\\_approach](https://www.researchgate.net/publication/334672402_Study_of_solidification_cracking_during_laser_welding_in_advanced_high_strength_steels_A_combined_experimental_and_numerical_approach), Accessed: 29-05-2024.
- [31] E. Doege, G. Dreyer, S. Ruesch, *Encyclopedia of Materials: Science and Technology* **2001**.
- [32] H. T, Z. X, *Materials Science and Engineering A* **2006**.
- [33] The Formation of Martensite | Total Materia, <https://www.totalmateria.com/articles/the-formation-of-martensite/>, Accessed: 29-05-2024.
- [34] The Properties and Effects of Manganese as an Alloying Element, [https://www\\_azom\\_com/article.aspx?ArticleID=13027](https://www_azom_com/article.aspx?ArticleID=13027), Accessed: 29-05-2024.
- [35] Plastics — Polyamide (PA) moulding and extrusion materials, Standard, International Organization for Standardization, Geneva, CH, **2022**.
- [36] R. Smallman, R. Bishop, *Modern Physical Metallurgy and Materials Engineering (Sixth Edition)* **1999**.
- [37] J. Thomason, *Composites Part A: Applied Science and Manufacturing* **2009**.
- [38] Y. Yoo, M. Spencer, D. Paul, *Polymer* **2011**.
- [39] Pigments for Plastics: Complete Technical Guide, <https://polymer-additives.specialchem.com/selection-guide/pigments-for-plastics>, Accessed: 27-05-2024.
- [40] Using Plastic Colorants To Brighten Your Injection Molded Parts, <https://revpart.com/using-plastic-colorants/>, Accessed: 27-05-2024.
- [41] T. A. Osswald, L.-S. Turng, PaulGramann, *ISBN-10: 3-446-40781-2* **2000**.
- [42] Y. Su, J. Zhu, X. Long, L. Zhao, C. Chen, C. Liu, *International Journal of Solids and Structures* **2023**.
- [43] P. G. Tallonaand, D. V. Malakhov, *CANADIAN METALLURGICAL QUARTERLY* **2021**.
- [44] K. Mao, D. Greenwood, R. Ramakrishnan, V. Goodship, C. Shrouti, D. Chetwynd, P. Langlois, *Wear* **2019**.
- [45] L. Zhang, Y. Zeng, H. Yao, Z. Shi, J. Chen, *Ceramics International* **2024**.

- [46] Ceramic Gears, <https://www.smallprecisiontools.com/en/products-solutions/ceramics-injection-molding/ceramic-applications/industrial-ceramic-parts/ceramic-gears1/>, Accessed: 27-05-2024.
- [47] A Comprehensive Guide to Ceramic CNC Machining, <https://www.runsom.com/blog/guide-to-ceramic-cnc-machining/>, Accessed: 27-05-2024.
- [48] Plastic Gears (Top Material Options), <https://www.sofeast.com/resources/materials-processes/internal-plastic-mechanical-parts-guides/plastic-gears/>, Accessed: 27-05-2024.
- [49] Exploring Different Types of Sintering Techniques: A Comprehensive Overview of 13 Methods, <https://www.xometry.com/resources/3d-printing/types-of-sintering/>, Accessed: 30-05-2024.
- [50] S. G. Hussein, *University of Baghdad 2019*.
- [51] Extrusion - An Overview of Metal Extrusion Process, <https://www.veryengineering.com/extrusion-an-overview-of-metal-extrusion-process/>, Accessed: 29-05-2024.
- [52] BGR - Mineralische Rohstoffe - Preismonitor Dezember 2019, [https://www.bgr.bund.de/DE/Themen/Min\\_rohstoffe/Produkte/Preisliste/pm\\_19\\_12.pdf](https://www.bgr.bund.de/DE/Themen/Min_rohstoffe/Produkte/Preisliste/pm_19_12.pdf), Accessed: 29-05-2024.
- [53] H. CL, B.-L. V, C. M, L. A, T. A, C. P., *Polymers 2020*.
- [54] R. C. T, *Physica A 2023*.
- [55] B. Bhattacharya, A. Chatterjee, Tuhin, K. Naskar, *Journal of Applied Polymer Science 2020*.
- [56] TPE vs. Silicone and Their Differences, <https://www.xometry.com/resources/materials/tpe-vs-silicone/>, Accessed: 29-05-2024.
- [57] J. Thomason, *Polymer Composites Volume 27 Issue 5 p. 552-562 2006*.
- [58] E. Kuram, *Journal of Composite Materials 2021*.
- [59] Y. Yoo, M. Spencer, D. Paul, *Polymer 2011*.
- [60] montmorillonite, <https://www.britannica.com/science/montmorillonite>, Accessed: 30-05-2024.
- [61] S. Mrzljak, A. Delp, A. Schlink, J.-C. Zarges, D. Hülsbusch, H.-P. Heim, F. Walther, *MDPI 2021*.
- [62] Comprehensive Guide on Polyamide (PA) or Nylon, Accessed: 29-05-2024.
- [63] H. Unal, *Materials Design 2004*.
- [64] Comprehensive Guide on Polycarbonate (PC), <https://omnexus.specialchem.com/selection-guide/polycarbonate-pc-plastic>, Accessed: 30-05-2024.